ELSEVIER

Thermochimica Acta 307 (1997) 1–10

thermochimica acta

The effects of structural recovery and thermal lag in temperature-modulated DSC measurements

Sindee L. Simon[a,*], Gregory B. McKenna[b]

[a] *Department of Chemical Engineering, University of Pittsburgh, Pittsburgh, PA 15261, USA*
[b] *Polymers Division, NIST, Gaithersburg, MD 20899, USA*

Received 13 March 1997; received in revised form 17 July 1997; accepted 31 July 1997

Abstract

It is well known that structural recovery in polymeric glass formers leads to the enthalpy overshoot in nonisothermal experiments. One common model for describing this phenomenon is the Tool–Narayanaswamy–Moynihan (TNM) equation. Here we apply the TNM equation to analyze a typical temperature-modulated DSC (TMDSC) trace and examine the influence of the material nonlinearities on the dynamic heat flow. We show that, in the glass-transition region, the oscillating heat-flow response to the sinusoidal temperature input is a distorted sine wave. Hence, linear analysis of the phase lag between heat flow and temperature is not physically meaningful. The degree of distortion of the sinusoidal heat flow increases as the magnitude of the excess enthalpy annealing peak increases. In addition, we perform a thermal analysis of samples having different geometries and show that an apparent phase lag can result in the measured response due to the presence of thermal gradients in the sample. The significance of the results is discussed. © 1997 Published by Elsevier Science B.V.

Keywords: Calorimetry; Dynamic calorimetry; Lissajous loops; Temperature-modulated DSC; Scanning calorimetry; Structural recovery; Tool–Narayanaswamy model

1. Introduction

Temperature-modulated differential scanning calorimetry (TMDSC) is a new technique in thermal analysis in which the normal temperature scan used in DSC is, generally, overlaid by a sinusoidal perturbation. The purported advantages of TMDSC include the ability to separate overlapping phenomena, as well as improved resolution and sensitivity. [1] However, analysis of the temperature-modulated differential scanning calorimetry (TMDSC) is currently the subject of debate. [1–3] One approach suggested by Schawe [3] involves a dynamic heat capacity analysis, similar to what one would obtain in dynamic mechanical measurements, i.e. one based on linear response theory. The phase angle between the sinusoidal heat flow and the sinusoidal temperature (or temperature derivative) is related to the loss in the system and is the parameter of interest. However, as Schawe notes, this approach is valid only if the response is linear. If the response is nonlinear, the heat flow will be a distorted sine wave, so that phase-angle measurements become meaningless. It is for this reason that the use of TMDSC to monitor nonlinear processes such as melting and reaction has been questioned [4]. One of the objectives of this paper is to show that the kinetics

*Corresponding author.

PII S0040-6031(97)00275-X

involved in structural recovery in the glass-transition region will make a linear analysis questionable in this region also.

There is a considerable body of work that models the impact of structural recovery on heat flow in standard DSC experiments in the glass-transition region [2,5–10]. The Tool–Narayanaswamy–Moynihan-type (TNM) models [5,6] have been very successful, not only in quantitatively predicting the material response to complex thermal histories, but also in providing a physical picture of the reasons for the behavior. The models are able to describe manifestations of glassy behavior including the rate-dependent glass temperature T_g, structural recovery, and the asymmetry of approach to equilibrium, the latter of which is due to the nonlinearity of structural recovery [11]. Of particular interest here is whether structural recovery and the nonlinearities, generally associated with it, should be considered in the analysis and application of temperature-modulated differential scanning calorimetry (TMDSC) measurements. Consequently, we perform model calculations for typical TMDSC thermal histories and investigate how the coupling between the thermal history and structural recovery impacts the TMDSC response as well as the interpretation of said response.

We summarize our results using Lissajous loops, which provide easy visualization of the degree of linearity between a sinusoidal input and the resulting output. To obtain a Lissajous loop, the response is plotted vs. the driving force. For a linear "viscoelastic" response, an elliptical pattern would be obtained. By analogy with dynamic mechanical measurements, the "elastic" in-phase component of the response is determined by the angle of the major axis of the ellipse. The "viscous" out-of-phase component of the response is related to the energy dissipated per cycle, which is equal to the area within the loop. A completely in-phase response will give a line, whereas a completely out-of-phase response will give a circle. If the response is nonlinear, the resulting Lissajous plot will be irregular in shape rather than elliptical. The linear response parameters for the material cannot be calculated when nonelliptic loops are observed. [12]

Lissajous loops have been used to test the quality of experimental TMDSC data by Wunderlich et al. [13,14]. In these works, quasi-isothermal experiments were performed in which the average temperature is held at a constant value for approximately twenty minutes while the heat-flow response to the oscillating temperature input is measured. The Lissajous plots were made by plotting heat flow vs. temperature, and generally showed wide, relatively stable ellipses at steady state. In what follows, we propose that the more appropriate variables for the Lissajous plot are heat flow vs. the instantaneous heating rate (dT/dt) rather than heat flow vs. temperature, since heat flow depends directly on the heating rate. The resulting plots yield direct information on the value of the apparent heat capacity.

Finally, we are interested in the effects of thermal lag on TMDSC results. Since the phase lag between the heat flow and the program temperature (or temperature derivative) is being measured, we are concerned that thermal gradients in the DSC sample will contribute to the apparent phase lag. To this end, we calculate the temperature profile in the DSC sample using the heat conduction equation and then perform model calculations with the thermal gradient incorporated.

2. Modeling TMDSC response in glass-forming materials

2.1. The material response equations

The output of TMDSC is simply heat flow as a function of time and/or temperature. We calculate the heat flow by noting that it is the time derivative of the enthalpy, which is, in turn, a function only of temperature in the equilibrium state (at constant pressure). In the glassy state, however, enthalpy is dependent on temperature and on the structure of the glass. A convenient measure of the structure of the glass is the fictive temperature, T_f, originally defined by Tool [15]. (T_f is defined as the temperature at which the enthalpy extrapolated along the glassy line would equal the equilibrium value.) Assuming that the enthalpy of the equilibrium liquid at zero Kelvin is zero, the enthalpy (H) of an amorphous material can be written as follows:

$$H = \int_{T}^{T_f} \Delta C_p \mathrm{d}T + \int_{0}^{T} C_{pl} \mathrm{d}T \tag{1}$$

where ΔC_p is the difference in heat capacity between the equilibrium (liquid) and glassy states ($C_{pl} - C_{pg}$), and C_{pl} is the equilibrium heat capacity. Here, in order to simplify calculations, we assume that the ΔC_p and C_{pl} are independent of time and temperature. Then, the enthalpy is given by:

$$H \equiv \Delta C_p(T_f - T) + C_{pl}T = \Delta C_p T_f + C_{pg}T \tag{2}$$

The heat flow (P) is simply the time derivative of the enthalpy:

$$P \equiv \frac{dH}{dt} = \Delta C_p \frac{dT_f}{dt} + C_{pg}\frac{dT}{dt} \tag{3}$$

This equation is equivalent to that derived by Moynihan [6].

For an ideal experiment, there is no thermal lag in the sample, and the instantaneous heating rate in the sample (dT/dt) would equal that of the program temperature. For this case, the problem of modeling the heat flow during a DSC temperature ramp is one of modeling the structural evolution of the material, i.e. $dT_f/dt = (dT_f/dT)\ (dT/dt)$. It is noted that, in a real TMDSC experiment, there is thermal lag in the sample and that this contributes to the measured phase lag. Here, we first develop the equations for an ideal TMDSC experiment with no thermal lag. We perform a thermal lag analysis in a subsequent section.

The Tool–Narayanaswamy model [5] accounts for the nonlinear behavior of glassy materials by including terms for the dependence of molecular mobility on glassy structure and for the nonexponential nature of structural (in this case enthalpy) recovery. Moynihan's formulation [6] of the Tool–Narayanaswamy model of structural relaxation (TNM model) is convenient because it yields the evolution of the fictive temperature for a given thermal history. A full description of the TNM formulation is given elsewhere [6]; only a brief description follows. According to the TNM model, the structural recovery process is represented by the generalized Kohlrausch [16]–William–Watts [17] (KWW) function:

$$\frac{dT_f}{dT} = 1 - \exp\left[-\left\{\int_0^t (dt/\tau_0)\right\}^{\beta}\right] \tag{4}$$

The nonexponentiality of the process is described by β; the nonlinearity is incorporated into the model by allowing the retardation time τ_0 to be a function not only of temperature but also of structure (T_f) (and hence a function of time). Eq. (4) can be solved numerically for a given thermal history which begins at a temperature T_0 above T_g:

$$T_{f,n} = T_0 + \sum_{i=1}^{n} \Delta T_i \left[1 - \exp\left(-\sum_{j=1}^{n} \frac{\Delta t_j}{\tau_{0,j}}\right)^{\beta}\right] \tag{5}$$

where $T_{f,n}$ is the fictive temperature after the nth temperature step, Δt_i the time step, and ΔT_i the temperature step (which is related to the time step by the instantaneous heating rate). Generally, it is found that time steps can be taken such that the temperature steps are 1 K in the equilibrium liquid regime and deep in the nonequilibrium glass; in the glass-transition region, where enthalpy recovery is observed, step sizes need to be reduced to 0.25 K or less [7]. To model the sinusoidal temperature history in TMDSC, we found that smaller step sizes must be used and that temperature steps of 0.05 K or less gave convergent results in all cases examined. The results presented here are for 0.05 K temperature steps.

A phenomenological equation relating the retardation time τ_0 to temperature and structure (T_f) is needed to perform the model calculations. The Tool–Narayanaswamy equation [5] is an Arrhenius-like equation, and is widely used:

$$\ln \tau_0 = \ln A + \frac{x\Delta h}{RT} + \frac{(1-x)\Delta h}{RT_f} \tag{6}$$

where the parameter x, introduced by Moynihan [6], partitions the material dependences between temperature and structure (T_f), and Δh and ln A are assumed to be constants. One problem with this equation is that it is unable to describe the observed Vogel [18] or Williams–Landel–Ferry [19] behavior in the equilibrium limit when $T_f = T$. However, since the Arrhenius behavior is approximately correct over a narrow temperature range and since the parameters have been obtained for several materials [7], it is used in the work described here.

2.2. The ideal TMDSC experiment

The evolution of the fictive temperature during a given thermal history is given by the solution of Eq. (4) coupled with an appropriate expression for

the relaxation time. The thermal history used for modeling an TMDSC experiment includes the cooling leg from above T_g to a point below T_g and the subsequent heating leg to above T_g. The temperature is generally temperature-modulated only in the heating leg. We first assume that no thermal lag is present such that the temperature of the sample is equal to the temperature of the furnace. The thermal history is then:

$$T = T_0 - qt \quad t \leq t_1 \tag{7}$$

$$T = T_0 - qt_1 + m(t - t_1) + A\sin[\omega(t - t_1)] \quad t > t_1 \tag{8}$$

where t_1 is the time at which the cooling leg is completed, q the cooling rate, m the heating rate, A the amplitude of the temperature modulation and ω the radian frequency of the modulation. For the heating leg, the instantaneous heating rate, which is used in Eq. (4) to compute the heat flow, is given by:

$$\frac{dT}{dt} = m + A\omega\cos[\omega(t - t_1)] \quad t > t_1 \tag{9}$$

2.3. The problem with thermal gradients included

For a real experiment, in which a thermal gradients exists, the heat flow given in Eq. (3) is calculated from the heating rate and fictive temperature both averaged over the entire sample:

$$P \equiv \frac{dH}{dt} = \Delta C_p \int_0^1 \frac{dT_f}{dt} d\xi + C_{pg} \int_0^1 \frac{dT}{dt} d\xi \tag{10}$$

where ξ is the dimensionless coordinate through the thickness of the sample ($= x/L$, where x is the thickness direction measured from the bottom of the sample and L the sample thickness).

To simplify calculations, we look at the effect of phase lag deep in the glassy state, where the first integral in Eq. (10) is zero since essentially no structural recovery occurs deep in the glass ($dT_f/dt = 0$). The second integral in Eq. (10) can then be determined by solving the one-dimensional heat conduction equation [20], in which radial heat transfer, given below, is neglected for the temperature profile:

$$\frac{\partial}{\partial x}\kappa\frac{\partial T}{\partial x} = \rho C_p \frac{\partial T}{\partial t} \tag{11}$$

where κ is the thermal conductivity, ρ the density, and C_p the heat capacity of the material. To solve the initial boundary value problem, the boundary conditions need to be specified. It is assumed that both the top and bottom of the sample are at the same temperature and a symmetrical gradient is present in the sample, i.e. the sample pan is assumed to be a perfect heat conductor, so that:

$$T(x = 0) = T_0 - qt_1 + m(t - t_1) + A\sin[\omega(t - t_1)] \quad t > t_1 \tag{12}$$

$$T(x = L) = T_0 - qt_1 + m(t - t_1) + A\sin[\omega(t - t_1)] \quad t > t_1 \tag{13}$$

The boundary value problem can be solved analytically for modulation at isothermal temperatures (where κ is a constant, $q = 0$, and $m = 0$). The solution is given by the following series:

$$T(x,t) = [T_0 + \sin(\omega t)] - \frac{4\omega L^2}{k}\sum_{n=1}^{\text{odd}} \frac{(n\pi)^2\cos(\omega t) + (\omega L^2/k)\sin(\omega t) - (n\pi)^2\exp(-(n\pi)^2 tk/L^2)}{n\pi[(n\pi)^4 + (\omega L^2/k)^2]}\sin\left(\frac{n\pi x}{L}\right) \tag{14}$$

where k is the thermal diffusivity $= \kappa/\rho C_p$. Eq. (14) can be inserted into Eq. (10) and integrated to give an analytical equation for the heat flow for the case in which there is a symmetrical thermal gradient in the sample and where $dT_f/dT = 0$:

$$P = C_{pg}A\left[\omega\cos(\omega t) + \frac{8\omega L^2}{k}\sum_{v=1}^{\text{odd}} \frac{\left((n\pi)^2\omega\sin(\omega t) - (\omega L^2/k)\omega\cos(\omega t) + \left(\frac{L^2}{k}\right)\exp(-(n\pi)^2 tk/L^2)\right)}{(n\pi)^2[(n\pi)^4 + (\omega L^2/k)^2]}\right] \tag{15}$$

An analytical solution can also be obtained in the rubbery state, where $dT_f/dT = dT/dt$. It is equivalent to Eq. (15) except that C_{pl} would replace C_{pg}.

3. Description of simulated experiments

3.1. Simulating ideal experiments

Calculations were performed for polystyrene and poly(vinyl chloride) assuming no thermal gradient for two cooling rates, 0.1 and 5.0°C min^{-1}. Typical of TMDSC experiments, the underlying heating rate was chosen to be 5°C min^{-1} in all calculations. The modulation amplitude and period ($= 2\pi/\omega$) were also taken to be typical values used in TMDSC experiments: 1°C and 60 s, respectively. Two cooling rates were used to demonstrate how the structural recovery on heating, which increases as the cooling rate decreases, results in distortions in the sinusoidal heat flow.

Polystyrene and poly(vinyl chloride) were used for the calculations presented here due to the large differences in the stated values of the nonlinearity parameter x and the nonexponential parameter β. The values used for $\Delta h/R$, x, β, and ln A, T_g, C_{pg} and C_{pl} are reported in Table 1 for the two materials. The values used are taken from the literature [7,21,22] with the exception of the heat capacity data for polystyrene, which was obtained in one of our laboratories [23].

3.2. Simulating experiments with thermal gradients

To determine the effects of thermal gradients, a quasi-isothermal TMDSC experiment was simulated in which the underlying heating rate is zero. Polystyrene was used for these calculations, and the modulation amplitude and period were again 1°C and 60 s, respectively. Calculations were performed at 50°C, deep in the glass, to demonstrate that an apparent phase lag may be observed experimentally due to thermal gradients in the sample in cases where the ideal calculations predict no phase lag. The physical parameters used to calculate the magnitude of the thermal gradient were: $\rho = 1.04\ g\ cm^{-3}$ [24], $\kappa = 1.17 \times 10^{-3}\ J\ cm^{-1}\ s^{-1}$ (by interpolation of literature data [25] to 50°C), and $C_{pg} = 1.52\ J\ g^{-1}\ K^{-1}$. Two sample sizes were considered: 0.05 and 0.2 cm thick.

4. Results and discussion

4.1. Lissajous loop analysis of ideal TMDSC experiment

Figs. 1 and 2 show the calculated Lissajous plots for an ideal (no thermal lag) polystyrene sample during heating in the TMDSC at 5°C/min after cooling at 5 and 0.1°C min^{-1}, respectively. Figs. 3 and 4 give analogous results for poly(vinyl chloride). Traditional Lissajous loops are made by plotting an output response vs. a driving signal. Here, we plot heat flow vs. the instantaneous heating rate (dT/dt), rather than

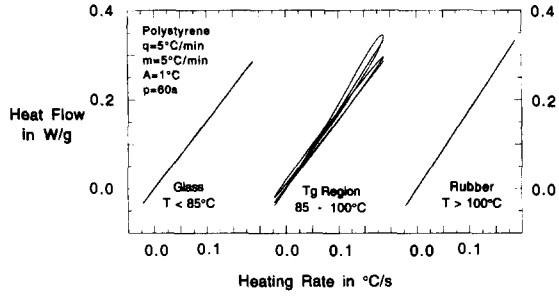

Fig. 1. Calculated Lissajous loops for polystyrene in three temperature regimes during TMDSC heating scans at 5°C/min after cooling at the same rate. Distortion of the oscillating heat flow is observed near T_g.

Table 1
Parameters used in model calculations

Material	T_g (K)	$\Delta h/R$ (K) [a]	x [a]	β [a]	ln (A/sec) [a]	C_{pg} (J g^{-1} K^{-1}) at T_g	C_{pl} (J g^{-1} K^{-1}) at T_g
Polystyrene	373.2 [b]	80,000	0.46	0.71	−216	1.52 [c]	1.77 [c]
Poly(vinyl chloride)	353.0 [a]	225,000	0.10	0.23	−622	1.12 [d]	1.43 [d]

[a] From Ref. [7].
[b] From Ref. [21].
[c] From Ref. [23].
[d] From Ref. [22].

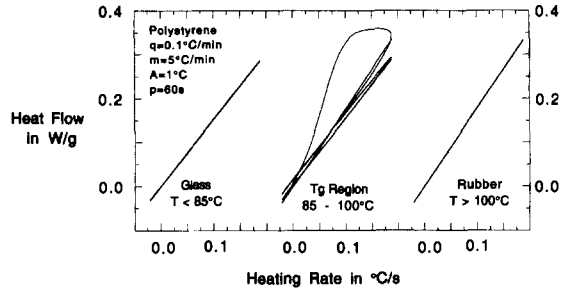

Fig. 2. Calculated Lissajous loops for polystyrene in three temperature regimes during TMDSC heating scans at 5°C/min after relatively slow cooling. Large distortions of the oscillating heat flow are observed near T_g.

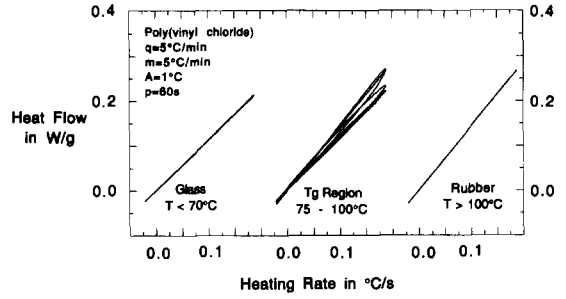

Fig. 3. Calculated Lissajous loops for poly(vinyl chloride) in three temperature regimes during TMDSC heating scans at 5°C/min after cooling at the same rate. Distortion of the oscillating heat flow is observed near T_g.

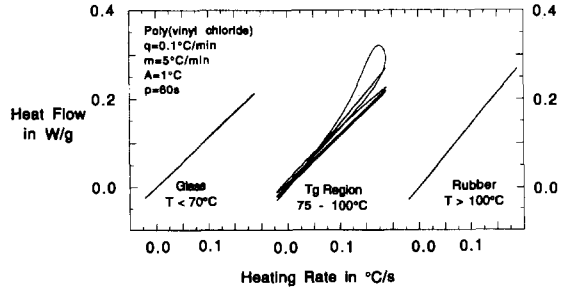

Fig. 4. Calculated Lissajous loops for poly(vinyl chloride) in three temperature regimes during TMDSC heating scans at 5°C/min after relatively slow cooling. Large distortions of the oscillating heat flow are observed near T_g.

heat flow vs. temperature as was done by Wunderlich [13,14]. The reason for this is that, based on Eq. (4), the heat flow should be in-phase with the instantaneous heating rate for a perfectly "elastic" response and a line with slope C_p would then be obtained on the Lissajous plot. An equivalent representation would be a plot of enthalpy vs. temperature, since enthalpy is in-phase with temperature for the perfectly "elastic" response. However, when heat flow is plotted vs. temperature, as in the work by Wunderlich [13,14], the perfectly "elastic" (in-phase) response gives a circle, indicating a phase lag of 90°C, if the traditional interpretation of the Lissajous plot is made. Furthermore, the heat capacity cannot be obtained directly from Wunderlich's loops, whereas, in our representation, the apparent heat capacity is equal to the slope of the loop analogous to viscoelasticity where the modulus is the slope of the stress vs. strain loop. Thus, although Wunderlich's representation is not incorrect, it does not directly yield as much information as our representation.

We note that our Lissajous loops are not centered about the zero point in the abscissa due to the underlying heating rate so that the loops go from $dT/dt = m + A\omega \cos(\omega t) = -0.021$ to 0.188°C/s. Later, when we show Lissajous loops for quasi-isothermal experiments (where $m = 0$), the Lissajous loops are centered about zero.

Figs. 1–4 each contain three plots, one in the glassy regime, one in the glass-transition region, and one in the rubbery regime. The Lissajous plot is a line in the glassy regime with a slope of C_{pg}. This can be understood by examining Eq. (4). In the glassy limit, where virtually no structural recovery occurs ($dT_f/dt \approx 0$), Eq. (4) reverts to:

$$P = C_{pg}\frac{dT}{dt} \tag{16}$$

Thus, in the glass, the heat flow and instantaneous heating rate are calculated to be in-phase for the ideal experiment. A similar result is obtained in the rubbery regime except that, in this case, the slope of the line is C_{pl} since $dT_f/dt = dT/dt$ in equilibrium so:

$$P = C_{pl}\frac{dT}{dt} \tag{17}$$

Examination of Figs. 1–4 and Eqs. (16) and (17) show a straightforward method to obtain heat capa-

cities deep in the glassy state and in the equilibrium-liquid regime from TMDSC results when no thermal lag is present in the sample. As shown later, however, thermal lag causes a decrease in the apparent heat capacity from the actual value.

In the glass-transition region, shown in the central part of each figure, the Lissajous loops show a progression of behaviors from a line with slope C_{pg} to distorted ellipses and then back to a line with slope C_{pl}. The distorted ellipses indicate that the oscillatory response is nonlinear in this (glass-transition) regime. The distortion is considerably larger for the slower cooling rate (Figs. 2 and 4) but it is present for both rates. Hence, it appears that the degree of distortion increases as the magnitude of the excess enthalpy annealing peak increases. This is reasonable because large excess enthalpy annealing peaks are accompanied by relatively large changes in the fictive temperature over a small temperature (or time) range. Hence, the term dT_f/dt in Eq. (3) changes rapidly from a value near 0 in the glass to a relatively large value when an excess enthalpy annealing peak is observed and then back to a value equal to dT/dt in the equilibrium liquid. The distortion in the sinusoidal heat flow is due to the fact that dT_f/dt is not in-phase with dT/dt when the excess enthalpy annealing peak occurs.

The distortions in the oscillatory heat flow can be seen more explicitly, although not as dramatically, in Fig. 5, where we plot the calculated heat flow as a function of time in the glass-transition region for polystyrene. Calculations were performed for a sample cooled at 0.1°C min^{-1} and heated at 5°C min^{-1}

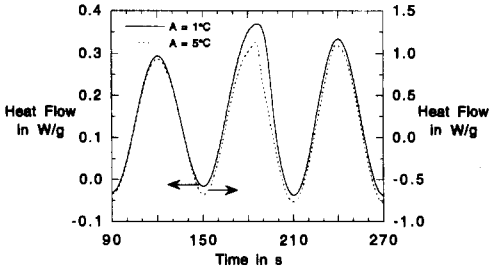

Fig. 5. Heat flow vs. time for polystyrene in the vicinit of T_g during heating at 5°C/min after cooling at 0.1°C/min. The amplitude of the oscilliatory temperature is 1°C and 5°C, respectively.

and for oscillatory temperature amplitudes of 1 and 5°C. The distortion of the sinusoidal heat flow increases as the amplitude of the temperature oscillation increases.

It is clear from the results in Figs. 1–5 that the oscillatory heat flow response in the glass-transition region can be highly nonlinear. When such distortions are present, the linear response parameters (i.e. C_p', C_p'', and tan δ) are obtained using a Fourier transform analysis and the phase lag δ is generally equated with the phase lag between the instantaneous heating rate and the first harmonic of the heat flow. If significant distortions are present, the resulting linear response parameters are not physically meaningful and cannot be quantitatively compared for different scans because their values depend on the degree of distortion present in the scans. This conclusion is corroborated by the fact that Wunderlich [13] observed that the breadth of the glass transition and the value of T_g obtained from the reversing heat flow (akin to C_p') changed systematically as the magnitude of the excess enthalpy annealing peak increased (i.e. as the degree of nonlinearity between the heat flow and instantaneous heating rate increased).

We have shown that the relationship between the heat flow and the instantaneous heating rate is nonlinear in the glass-transition region. It is less clear how the Tool–Narayanaswamy parameters influence the strength of the nonlinearity of the response (i.e. the degree of distortion in the Lissajous plot). The parameter β represents the width of the retardation spectrum, and intuitively, it seems it should not impact the material's nonlinear response. On the other hand, it would seem that the parameter x should impact the nonlinear response since x partitions the temperature and structure dependences of the retardation time. Yet in our calculations, poly(vinyl chloride), which has a small x (large structure dependence) shows less distortion of the Lissajous loops in the glass-transition region than does polystyrene. Hence, it appears that there is a complex coupling between structure dependence, width of the retardation spectrum, and experimental conditions that determines the impact of structural recovery on the TMDSC response upon traversing the T_g region. We speculate that it is the breadth of the glass transition of poly(vinyl chloride), as reflected in the wide spectrum of retardation times (low β), that dampens the nonlinear response under

the experimental conditions chosen for simulation in this study.

Calculations we performed with $x = 1$, and all other parameters equal to those used for Fig. 2, still showed distorted Lissajous loops through the glass transition although the distortions were smaller and similar to those shown in Fig. 1. Thus, the nonlinearity of structural recovery need not be present to obtain the nonlinear relationship between the heat flow and the temperature. Rather, what seems to be necessary is the nonlinear temperature dependence of τ_0. The strength of the distortions in the heat flow then arise from a complex coupling between the nonlinear material behavior, the width of the retardation spectrum, and the experimental conditions.

This point is consistent with the results of Hutchinson and Montserrat [26] who performed similar calculations using a simple exponential function ($\beta = 1$ in the KWW equation) but did not report observing the nonlinear responses seen here. Based on our calculations, where we used $\beta = 1$ and faster cooling rates, the reason for the differences from our results is that Hutchinson and Montserrat chose cooling and heating conditions ($q = 20°C\ min^{-1}$ and $m = 2.5°C\ min^{-1}$) which result in no enthalpy overshoot and, hence, little distortion in the sinusoidal heat flow and the resulting Lissajous loop. This implies that the selection of thermal histories chosen for TMDSC measurements through the glass transition is governed by different criteria than is the same selection for untemperature-modulated DSC. In untemperature-modulated DSC, it has been recommended [27] that the heating and cooling rates be the same or that the heating rate be faster than the cooling rate to avoid physical aging during heating. The conditions studied in this paper conform to this set of criteria but resulted in nonlinearities that make the linear analysis applied to TMDSC results questionable. On the other hand, for a condition in which the cooling rate is eight times the heating rate, nonlinearities are much smaller and a linear analysis may be more appropriate. The selection of thermal histories for TMDSC to avoid the nonlinearities seen here is beyond the scope of this work.

4.2. *Thermal gradient effects*

Finally, we examine the effects of thermal gradients on apparent phase lag in the TMDSC experiments.

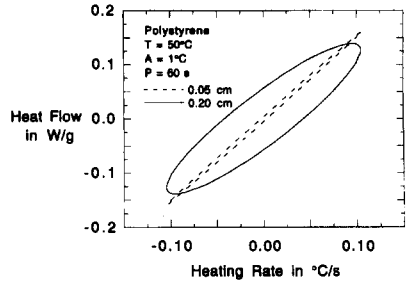

Fig. 6. Lissajous loops calculated taking thermal lag into consideration for polystyrene during a quasi-isothermal TMDSC experiment at 50°C for samples 0.05 and 0.20 cm thick, respectively.

Fig. 6 shows two Lissajous loops obtained for glassy polystyrene at 50°C in a simulated quasi-isothermal experiment in which thermal gradients are present in the sample. The two loops correspond to samples of different sizes: one 0.05 cm thick and the other 0.20 cm thick. The phase lag between the heat flow and the heating rate is greater in the thicker sample due to the larger thermal gradient. Hence, the Lissajous loop of the thicker sample is broader. In neither case is the simple line with slope C_{pg} and zero width, which we observed for the ideal TMDSC experiment in the glassy state in Figs. 1–4, obtained. However, an apparent heat capacity can be obtained from the slope of the loops shown in Fig. 6. This apparent heat capacity does not equal the true heat capacity, but decreases as the thermal lag increases. For the sample of thickness 0.05 cm, the average phase lag between the heat flow and the heating rate is less than 1 deg (0.0028 radians) and the slope of the loop is $1.519\ J\ g^{-1}\ K^{-1}$, nearly equivalent to the C_{pg} input ($1.52\ J\ g^{-1}\ K^{-1}$) to the simulations. However, for the sample of thickness 0.20 cm, the average phase lag is 12 deg and the slope of the loop is $1.19\ J\ g^{-1}\ K^{-1}$, which would give an error of 22% in the heat capacity. We note that such errors will be larger in the melt state where the thermal conductivity of the material is lower and thermal gradients are larger than in the glass. These calculated results are corroborated by the experimental work of Marcus and Blaine who have noted that the decrease in the apparent heat capacity for thicker samples is related to the thermal conductivity. [28]

It is emphasized that the results presented in Figs. 1–6 are simulations. Experimental verification is needed. We also note that TMDSC may provide a tool to explore the reasons for the fact that the Tool–Narayanaswamy–type models do not fully represent the nonlinear response of glass-forming materials [7,10,29].

5. Conclusions

The temperature-modulated DSC experiment for two glassy polymers, polystyrene and poly(vinyl chloride) was analyzed in the context of the Tool–Narayanaswamy–Moynihan model of structural recovery. Using a Lissajous loop analysis, we demonstrate that the oscillating heat flow becomes a distorted sine wave in the vicinity of the glass. The degree of distortion increases as the magnitude of the excess enthalpy annealing peak increases. These results demonstrate that a linear analysis of the TMDSC experiment, as suggested by Schawe [3], will not be valid in this region under the conditions analyzed here.

We also find that the material parameters used in the Tool–Narayanaswamy–Moynihan model [5,6] affect the degree of distortion observed in the Lissajous loop in the vicinity of T_g. Surprisingly, the magnitude of the loop distortion was greater for the polystyrene than for poly(vinyl chloride), in spite of the fact that poly(vinyl chloride) has a larger nonlinearity parameter x (i.e. the structure dependence of the relaxation time is larger). At the same time, polystyrene shows a narrower distribution of relaxation times, indicating that the distortion of the sinusoidal heat flow is dampened by the broader relaxation spectrum of the poly(vinyl chloride).

The ideal material analysis, without incorporating thermal lag, shows that the heat capacity of the materials deep in the glass and in the equilibrium liquid state can be obtained directly from the slope of the major axis of the Lissajous plot of dH/dt vs. dT/dt. However, when thermal gradients are present in the sample, the slope of the Lissajous loop decreases and its width increases. For a 0.05 cm thick polystyrene sample, the error in the apparent heat was calculated to be $< 0.1\%$. As the sample thickness increases, however, the apparent heat capacity calculated from the slope of the Lissajous loop decreases and is 22% too low for a sample having a 0.20 cm thickness.

The results obtained in this paper demonstrate that TMDSC, while a potentially useful new analytical tool, needs to be used with caution when analyzing materials in the vicinity of T_g, where nonlinearities occur and when using sample thicknesses typical of untemperature-modulated DSC samples because thermal lag affects the apparent heat capacity and phase lag.

References

[1] M. Reading, TRIP 1 (1993) 248.
[2] B. Wunderlich, Y. Jin, A. Boller, Thermochim. Acta 238 (1994) 277.
[3] J.E.K. Schawe, Thermochim. Acta 271 (1996) 127.
[4] T. Ozawa, K. Kanari, Thermochim. Acta 252 (1995) 183.
[5] O.S. Narayanaswamy, J. Am. Ceram. Soc. 54 (1971) 491.
[6] C.T. Moynihan, P.B. Macedo, C.J. Montrose, P.K. Gupta, M.A. DeBolt, J.F. Dill, B.E. Dom, P.W. Drake, A.J. Easteal, P.B. Elterman, R.P. Moeller, H. Sasabe, J.A. Wilder, Ann. N.Y. Acad. Sci. 279 (1976) 15.
[7] I.M. Hodge, J. Non-Cryst. Solids 169 (1994) 211.
[8] J.M. O'Reilly, CRC Crit. Rev. in Solid State and Mat. Sci. 13 (1987) 259.
[9] R.W. Rendell, J.J. Aklonis, K.L. Ngai, G.R. Fong, Macromolecules 20 (1987) 1070.
[10] G.B. McKenna, in Comprehensive Polymer Science, Volume 12, Polymer Properties, C. Booth, C. Price (Eds.), Pergamon, Oxford (1989), p. 311.
[11] A.J. Kovacs, Ann. N.Y. Acad. Sci. 371 (1981) 38.
[12] Frank Filisko, in: K.O. Havelka, F.E. Filisko (Eds.), Progress in Electrorheology, Plenum Press, New York, 1994.
[13] A. Boller, C. Schick, B. Wunderlich, Thermochim. Acta 266 (1995) 97.
[14] A. Boller, Y. Jin, B. Wunderlich, J. Ther. Anal. 42 (1994) 307.
[15] A.Q. Tool, J. Am. Ceram. Soc. 29 (1946) 240.
[16] R. Kohlrausch, Pogg. Ann. Phys. 91 (1854) 198.
[17] G. Williams, D.C. Watts, Trans. Faraday Soc. 66 (1970) 80.
[18] H. Vogel, Phys. Z. 22 (1921) 645.
[19] M.L. Williams, R.F. Landell, J.D. Ferry, J. Am. Chem. Soc. 77 (1955) 3701.
[20] W.E. Boyce, R.C. DiPrima, Elementary Differential Equations and Boundary Value Problems, John Wiley and Sons, New York, 1986.
[21] T.G. Fox, P.J. Flory, J. Appl. Phys. 21 (1950) 581.
[22] U. Gaur, B.B. Wunderlich, B. Wunderlich, J. Phys. Chem. Ref. Data 12 (1983) 29.

[23] S.L. Simon, D.J. Plazek, T. Holden, unpublished data.
[24] Robert A. Orwoll, in: Mark, (Ed.), Physical Propeties of Polymers Handbook, American Institute of Physics, Woodbury, NY (1996), Chap. 7, p. 81.
[25] Yong Yang, in: Mark, (Ed.), Physical Propeties of Polymers Handbook, American Institute of Physics, Woodbury, NY (1996), Chap. 9, p. 111.
[26] J.M. Hutchinson, S. Montserrat, J. Therm. Anal. 47 (1996) 103.
[27] A.J. Kovacs, J.M. Hutchinson, J. Polym. Sci., Polym. Phys. Ed. 17 (1979) 2031.
[28] S.M. Marcus, R.L. Blaine, Thermochim. Acta 243 (1994) 231.
[29] G.B. McKenna, C.A. Angell, J. Non-Cryst. Sol. 528 (1991) 133–133.